



AIAA

**Feasibility Study of an Adaptive
Large Eddy Simulation Method**

Daniel E. Goldstein and Oleg V. Vasilyev
Mechanical Engineering Department,
University of Colorado-Boulder,
UCB 427, Boulder, CO 80309-0427

Nicholas K. R. Kevlahan
Department of Mathematics & Statistics,
McMaster University
Hamilton, ON Canada L8S 4K1

**16th AIAA Computational Fluid Dynamics
Conference
June 23–26, 2003/Orlando, Florida**

Feasibility Study of an Adaptive Large Eddy Simulation Method

Daniel E. Goldstein and Oleg V. Vasilyev
*Mechanical Engineering Department,
University of Colorado-Boulder,
UCB 427, Boulder, CO 80309-0427*

Nicholas K. R. Kevlahan
*Department of Mathematics & Statistics,
McMaster University
Hamilton, ON Canada L8S 4K1*

A novel method for simulating turbulent flows called Stochastic Coherent Adaptive Large Eddy Simulation (SCALES) is introduced. The theoretical basis for SCALES is presented using results from *a priori* testing of homogenous turbulence along with a novel Coherency Diagram of a turbulent field that physically relates Direct Numerical Simulation to different Large Eddy capturing methods, such as SCALES, CVS, LES and VLES. Results from *a priori* testing show that given the same compression ratio the SCALES method will result in a significantly lower level of subgrid scale dissipation that needs to be modeled in comparison to LES. The feasibility of SCALES is demonstrated by considering numerical simulations of two dimensional flow around a cylinder for Reynolds numbers in the range $3 \times 10^1 \leq Re \leq 10^5$ using an adaptive wavelet collocation method. It is demonstrated in actual dynamic simulations that the compression scales like $Re^{1/2}$ over five orders of magnitude, while computational complexity scales like Re . This represents a significant improvement over the naive complexity estimate of $Re^{9/4}$ for two-dimensional turbulence.

Introduction

The problem of simulating high Reynolds number (Re) turbulent flows of engineering and scientific interest would have essentially been solved with the advent of Direct Numerical Simulation (DNS) techniques if unlimited computing power, memory, and time could be applied to each particular problem. Yet given the current and near future computational resources that exist and a reasonable limit on the amount of time an engineer or scientist can wait for a result, the DNS technique will not be useful for more than unit or benchmark problems for the foreseeable future.^{1,2} The high computational cost for the DNS of three dimensional turbulent flows results from the fact that they have eddies of significant energy in a range of scales from the characteristic length scale of the flow all the way down to the Kolmogorov length scale. Because of the large disparity in scales that need to be fully resolved, the actual cost of doing a three dimensional DNS scales as $Re^{9/4}$. Fortunately, because the eddies are localized in space and scale, there is a possibility of “compressing” the problem. This localization can be exploited by locally compressing the

problem such that all the modes from the characteristic length scale down to the Kolmogorov length scale are still resolved. This can be achieved by applying a recently developed dynamically adaptive wavelet collocation method³⁻⁵ to the solution of the Navier–Stokes equations. The wavelet collocation method employs wavelet compression as an integral part of the solution such that the solution is obtained with the minimum number of grid points for a given accuracy. When the threshold is chosen simply to satisfy numerical accuracy (and subgrid scales are not modeled) we call this method wavelet based direct numerical simulation, or WDNS. It has been shown recently⁵ that in WDNS simulations of two dimensional flows the computational complexity scales like Re . The extension to three dimensional turbulence is currently underway. In this paper we propose a novel approach called the Stochastic Coherent Adaptive Large Eddy Simulation (SCALES) method. This method uses the dynamically adaptive wavelet collocation method to simulate turbulence with a significantly higher compression ratio than WDNS and Coherent Vortex Simulation (CVS).⁶ We will show that SCALES combines the advantages of both CVS and LES such that the minimum number of modes are resolved in the simulation, given the maximum acceptable simulation error. We will also show that given the same compression ratio the SCALES method produces a significantly lower level of subgrid

Copyright © 2003 by the American Institute of Aeronautics and Astronautics, Inc. No copyright is asserted in the United States under Title 17, U.S. Code. The U.S. Government has a royalty-free license to exercise all rights under the copyright claimed herein for Governmental Purposes. All other rights are reserved by the copyright owner.

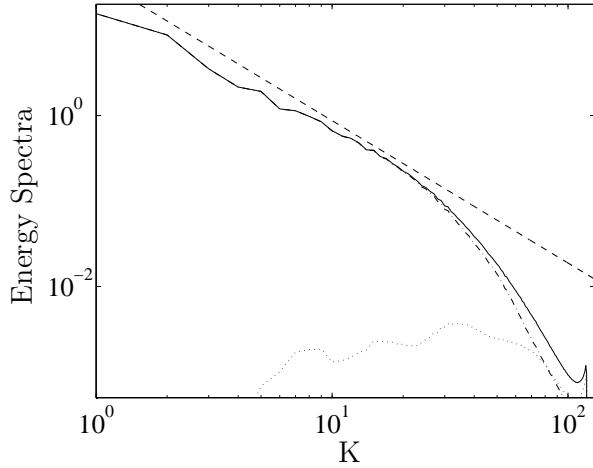


Fig. 1 Wavelet filtering applied to DNS of forced homogeneous turbulence (field: F_{256}) wavelet filtered at CVS compression (95.0%) using LI6 wavelets. DNS field (—). Filtered field using LI6 wavelets(CVS compression 95%) : (---), Residual field: (.....), $K^{-5/3}$ line: (-.-.-)

scale dissipation compared to LES. This is important since subgrid scale dissipation must be modelled.

In this paper we first discuss reduced order methods for simulating turbulent flows. We will then briefly present the Coherent Vortex Method. Following this we will present *a priori* results, using DNS of forced homogeneous turbulence, to illustrate the important characteristics of the wavelet thresholding filter. A novel Coherency Diagram of a turbulent field is then presented to physically relate DNS and WDNS to different large eddy capturing methods, such as CVS, LES and VLES. The Stochastic Coherent Adaptive Large Eddy Simulation (SCALES) method is then presented in the context of the Coherency Diagram. A brief overview of the dynamically adaptive wavelet collocation algorithm is then presented along with two dimensional WDNS results for flow around a fixed cylinder for $3 \times 10^1 \leq Re \leq 10^5$. These results are shown to highlight this methods ability to dynamically adapt the computational grid to resolve the energetic structures in a turbulent flow.

Background

Since computing power, memory, and time are all scarce resources, the problem of simulating turbulence has become one of how to abstract or simplify the complexity of the physics represented in the full Navier–Stokes (NS) equations in such a way that the important physics of the problem is approximated at a lower cost. To do this, a portion of the modes of the turbulent flow field is approximated by a low order model that is cheaper than the full NS calculation. This model can then be used along with a numerical simulation of the important modes of the problem that cannot be well represented by the model. The decision

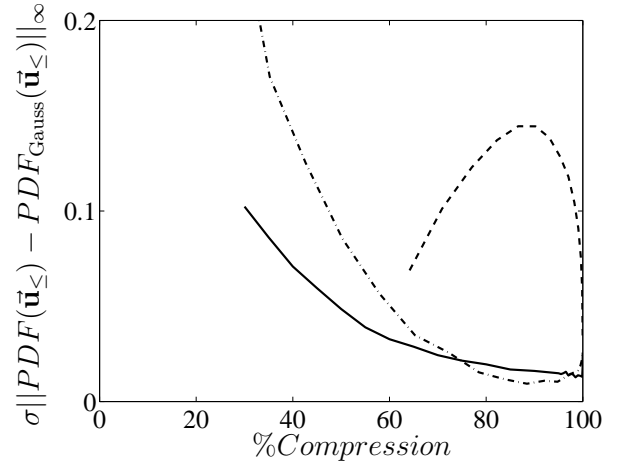


Fig. 2 Normalized L_∞ -error between SGS field and Gaussian PDFs with the same mean and variance. Wavelet filter applied to: velocity (—), vorticity (---). Fourier filter (-.-.-).

of what part of the physics to model and what kind of model to use must be based on what physical properties are considered important for the problem. It should be noted that nothing is free, so any use of a low order model will by definition lose some information about the original flow.

In an abstract sense, the first question to address when one is looking to develop a reduced order method for simulating turbulent flows is to determine which parts of the physical system will be approximated with a low order model and which parts will be simulated numerically. One choice is to use time averages: this technique is used in Reynolds Averaged Navier–Stokes (RANS) simulations.⁷ Another option is to view the turbulent flow as a set of flow structures moving in a Lagrangian frame and then track their interactions over time. This approach has been used in vortex simulation methods.⁸ Yet another option is to simulate the flow on an adapted grid that is coarser than the grid necessary to represent the flow down to the Kolmogorov length scale. The goal of this type of method is to resolve the energetic eddies that dominate the flow physics. Any coarsening of the grid, either locally or globally, implies that not all the modes or frequencies of the original flow are resolved. These missing modes have to be modeled somehow. In this class of methods we will also include Galerkin⁹ methods that approximate the problem on a reduced set of basis functions. We will refer to this class of methods as Eddy Capturing Methods.

Large Eddy Simulation

The dominant method in the class of Eddy Capturing Methods is Large Eddy Simulation (LES). The motivation behind LES is the recognition that the large scales of the turbulence often dominate mixing, heat transfer and other quantities of engineering in-

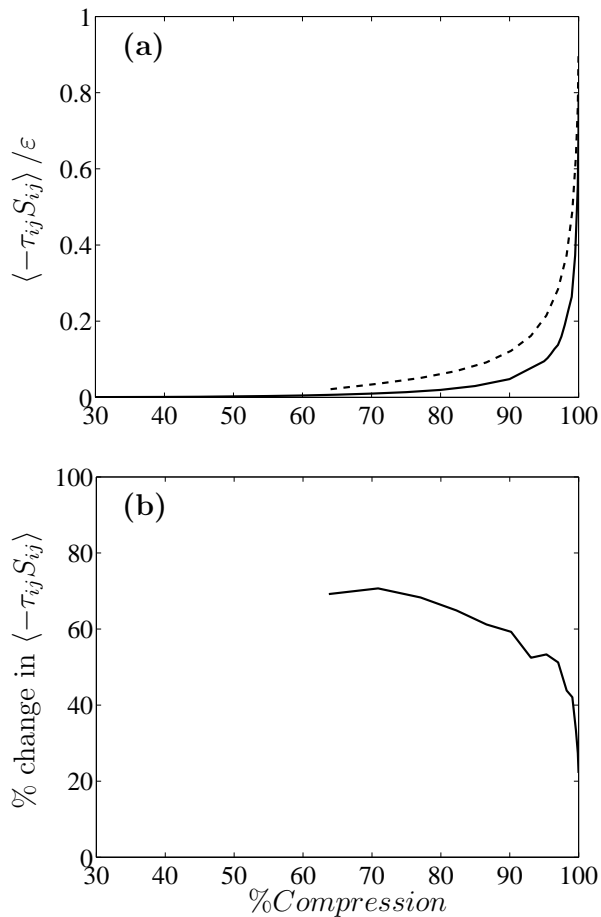


Fig. 3 (a) Mean subgrid scale dissipation normalized by the full field mean viscous dissipation, $\epsilon = \langle 2\nu S_{ij} S_{ij} \rangle$. Wavelet filter applied to: velocity (—). Fourier filter (----). (b) % difference in mean subgrid scale dissipation between wavelet filtering and Fourier filtering.

terest, while the small scales are of interest only via their effect on the large scales. The incompressible LES equations describing the evolution of the large scale eddies in the flow field are

$$\frac{\partial \bar{u}_i}{\partial x_i} = 0, \quad (1)$$

$$\frac{\partial \bar{u}_i}{\partial t} + \frac{\partial (\bar{u}_i \bar{u}_j)}{\partial x_j} = -\frac{1}{\rho} \frac{\partial \bar{p}}{\partial x_i} + \nu \frac{\partial^2 \bar{u}_i}{\partial x_j \partial x_j} + \frac{\partial \tau_{ij}}{\partial x_j}, \quad (2)$$

where

$$\tau_{ij} = \bar{u}_i \bar{u}_j - \bar{u}_i \bar{u}_j. \quad (3)$$

As a result of the filtering process the unresolved quantity τ_{ij} , commonly referred to as the Subgrid Scale (SGS) stress, is introduced. Note that τ_{ij} is a function of the unfiltered field u_i . However, to realize the benefit of LES a low order model for the SGS stress, which is based on the resolved quantities, is needed. In practice τ_{ij} can be modeled either deterministically or stochastically. Most current LES is done using purely deterministic models.¹⁰⁻¹² The current research efforts

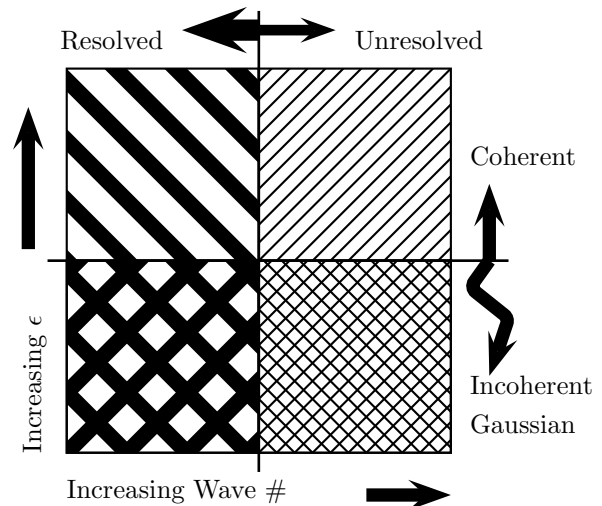


Fig. 4 Coherency Diagram of turbulent field

in LES involve finding improved SGS stress models for τ_{ij} .

The problem with LES is that it resolves the large scale eddies (i.e. small wavenumbers) instead of the actual coherent vortices. It has been shown that the coherent vortices in a turbulent flow contain significant energy at all length scales from the characteristic length scale of the domain down to the Kolmogorov length scale.¹³⁻¹⁶ In Ref. 17 a visual study of the physical structure of turbulence is presented. The authors conclude that the *vorticity tubes, which seem to be the basic structure of three-dimensional homogeneous turbulence, involve all the scales of the flow.* Because vortices are multi-scale, when a spectral cutoff filter is used with LES the small scale structure of the coherent energetic eddies are not resolved. Therefore the small scale part of the vortices must be modeled. However, the hypothesis behind most LES subgrid stress models is that the subgrid scales being modeled have a generally universal character.^{18,19}

Another problem with LES is that the computational grid is commonly defined *a priori* based on the physics and geometry of the problem.^{12,20,21} Yet in flow problems of engineering and scientific interest the large scales of interest often change over the domain of the problem and in time. As Pope states in his recent book on turbulence¹⁹ *the ideal numerical method for LES would include adaptive gridding to ensure automatically that the grid, and hence the filter, are everywhere sufficiently fine to resolve the energy-containing motions.* This implies that the Eddy Capturing Method should be adaptive in time and space.

Coherent Vortex Simulation

A relatively new method in the class of Eddy Capturing Methods is the Coherent Vortex Simulation⁶ (CVS) method. CVS is based on the observation that an orthogonal wavelet filter, when applied to a turbulent vorticity field, can decompose it into the resolved

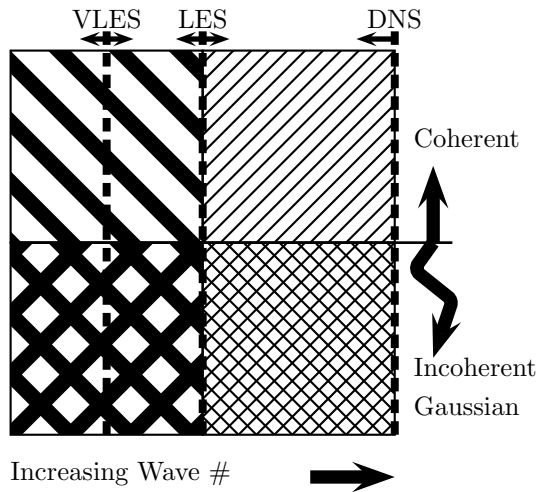


Fig. 5 Coherency Diagram of turbulent field for DNS, VLES and LES

field that contains the coherent vortices, and the residual, or subgrid field, which is purely incoherent and has near Gaussian statistics. We define CVS compression as the wavelet compression level where the incoherent subgrid field is most Gaussian. In theory, if the subgrid field is purely incoherent Gaussian white noise, the total SGS dissipation would be zero. Therefore the SGS stress model for a CVS simulation could be purely stochastic. The main problem with the CVS method is that the wavelet compression that results in a Gaussian subgrid field can be difficult to determine during an actual simulation. Even if it can be found in a cost effective manner, it is likely that the associated adapted grid will be too fine to be cost effective for simulating high Re number flows.

In this work we show that a second generation bi-orthogonal wavelet filter is able to accomplish this coherent/incoherent decomposition with both a velocity and a vorticity field. The *a priori* results presented in this work use second generation lifted interpolating wavelets²² of order 6 that are also used in the fully adaptive wavelet collocation method³⁻⁵ discussed briefly below. (Note we will refer to this family of wavelets as LI6 wavelets)

Velocity decomposition is of particular interest in studying different Eddy Capturing Methods because it allows us to directly calculate the SGS dissipation after applying the wavelet filter. Figure 1 shows the energy spectra of an isotropic turbulence field decomposed into coherent/incoherent parts. In Figure 2 we present the L_∞ -error (scaled by the standard deviation) between the probability density function of the subgrid scale field and a Gaussian PDF with the same mean and variance. Three different filter types are compared. We can see from this figure that there exists a compression where the L_∞ -error is minimized. For vorticity filtering this minimum occurs at a compression of 90%, whereas for velocity filtering this

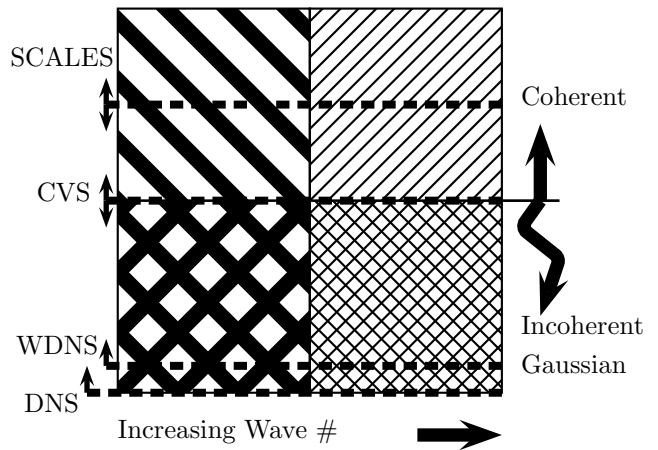


Fig. 6 Coherency Diagram of turbulent field for WDNS, DNS, CVS and SCALES

minimum occurs at a higher compression of 99.5%. In contrast using a Fourier filter results in an error trace that is concave downward.

As stated above, velocity wavelet filtering allows us to directly calculate the SGS dissipation after applying the wavelet filter. Figure 3(a) shows the total subgrid stress dissipation normalized by the DNS viscous stress dissipation for the wavelet and Fourier filter applied to the velocity field. Both filters produce a total subgrid stress dissipation that increases with compression. But with the wavelet filter the total subgrid stress dissipation stays flat relatively longer than with the Fourier filter. This difference suggests one advantage of using the wavelet filter: for a given compression ratio the subgrid stress dissipation is less than when a Fourier filter is used. Thus, the subgrid scale should have a smaller effect when using wavelet filters. To quantify this difference, Fig. 3(b) shows the percent difference between the total subgrid scale dissipation with the wavelet and the Fourier filters. We see that the largest difference is at 70% compression where the wavelet filter results in a SGS dissipation 70% lower in comparison to using the Fourier cutoff filter. In the region of compression that is of more interest for actual simulations we see that the difference is still significant. At 95% compression the difference using the wavelet filter is still 50%. So in terms of maximizing the compression while minimizing the mean SGS dissipation we find that 95% compression is optimal. This can be considered a more direct way to define the CVS compression since in CVS ultimately we are concerned with minimizing the total SGS dissipation.

Coherency Diagram

A key part of this work has been to understand different filter types and their effect on the physical interaction between the residual and filtered fields in large eddy capturing methods such as LES and CVS.

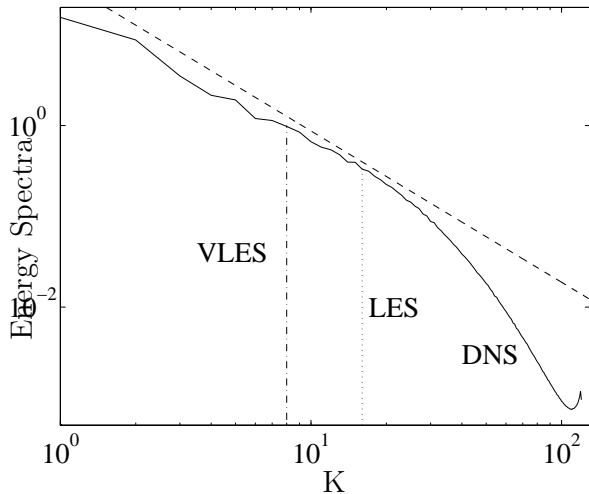


Fig. 7 DNS field (—), VLES filtered field (---) and LES filtered field (.....).

To do this, a Coherency Diagram of a turbulent field in terms of wave number and wavelet threshold ϵ has been developed (see Fig. 4). In this figure a vertical line can be thought of as dividing the field into resolved (below the cutoff wave number) and residual (above the cutoff wave number) fields. This is of course the result of explicitly applying a Fourier cutoff filter to the field. It is also the result of representing the field on a reduced regular grid, thus implicitly filtering the field. Now the same field can be separated by applying a wavelet thresholding filter. In Fig. 4 this is represented by drawing a horizontal line across the square at a given wavelet filter threshold of ϵ . As discussed earlier, there exists an ϵ such that the square can be divided into coherent and incoherent parts (this is the ϵ used in CVS). Now from this Coherency Diagram it can be seen immediately that when the field is separated using a Fourier cutoff filter the resulting subgrid contains both coherent and incoherent parts.

In Fig. 5 the vertical lines of separation on the Coherency Diagram for DNS, LES and VLES are shown. First it is clear that in DNS there is no subgrid (by definition) so the separation line is at the highest wave number needed to capture the physics of the turbulent field down to the Kolmogorov scale. Then the vertical line for LES is shown that divides the field at some Fourier cutoff value, usually taken to be in the inertial range. At an even lower wave number we have the vertical separation line for Very Large Eddy Simulation. Figure 7 shows the energy spectra of a DNS of homogeneous/isotropic turbulence. This turbulent field was obtained from a 256^3 DNS simulation of forced homogeneous/isotropic turbulence¹³ with $Re_\lambda = 168$ and will hereafter be referred to as F_{256} . The energy spectra after a LES and a VLES Fourier cutoff filter is applied are also shown.

figure

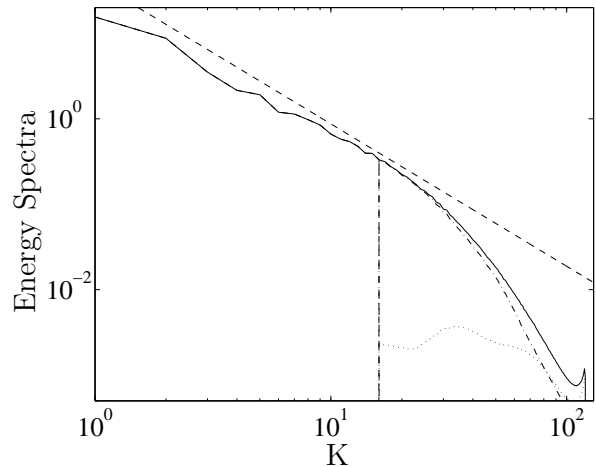


Fig. 8 DNS field (—), SCLES resolved field is same as DNS up to $K_c=16$ as in LES. Coherent part of subgrid field: $(u_{> cvs})'$ (— · —). Incoherent part of subgrid field: $(u_{< cvs})'$ (.....).

Stochastic Coherent Large Eddy Simulation

When developing Large Eddy Simulation (LES) subgrid stress models the assumption is usually made that the filtering operation separates the large eddies from the smaller eddies, and that the resulting residual subgrid field is largely stochastic in nature. Another way of saying this is that the coherent structures are being separated from the incoherent structures. Now in terms of the regions of Coherency Diagram discussed above (see Figs. 4 and 5) it is clear that the LES subgrid does contain coherent structures in an incoherent background. In Fig. 8 we present the energy spectra of a forced DNS turbulence field and the coherent $(u_{> cvs})'$ and incoherent $(u_{< cvs})'$ parts of the SGS field. To accomplish this decomposition of the LES SGS field we used a LI6 wavelet filter. The wavelet threshold ϵ that results in CVS compression of 95% for this field is used (see Fig. 1). It can be seen clearly that there is significant energy in the coherent part of the SGS.

In developing or evaluating a LES model one of the quantities of particular interest is the SGS dissipation. In Fig. 9 we present the probability density function (PDF) of the SGS dissipation $(-\tau_{ij}\bar{S}_{ij})$ for the full SGS after the application of a Fourier cutoff filter ($K_c = 16$), along with the coherent SGS and the incoherent SGS. The subgrid stress (τ_{ij}) is decomposed into the contributions from the coherent and the incoherent parts of τ_{ij} , using $(u_{> cvs})'$ and $(u_{< cvs})'$, while \bar{S}_{ij} is calculated from the resolved field in all three cases. Back-scatter (i.e. energy transfer from the SGS to the resolved scales) on the PDF plot is in the negative direction on the horizontal axis. We emphasize that in SCLES the PDF of the full and the coherent SGS dissipation are nearly identi-

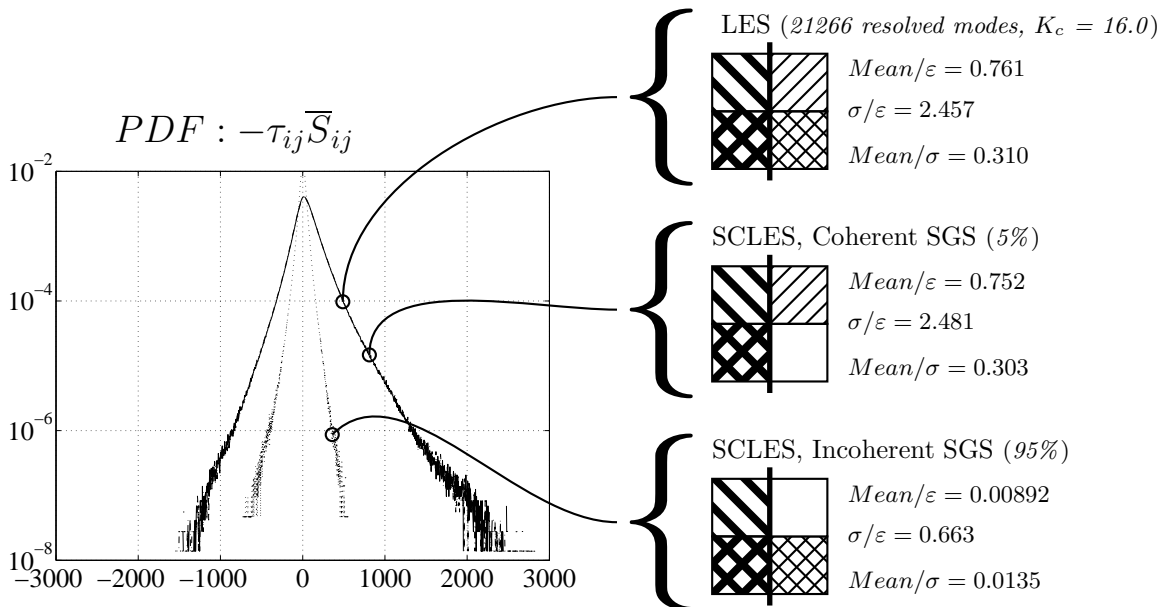


Fig. 9 SCLES subgrid scale dissipation for homogeneous turbulence field F_{256} . Fourier cutoff filter ($K_c = 16$) is used along with a velocity field wavelet filter using LI6 wavelets.

cal, even though the coherent SGS contains only 5% of the modes of the original subgrid field. In both cases it can be seen that the mean of the PDF is positive. This shows that there is both forward and back-scatter but the net SGS dissipation is positive. The incoherent SGS dissipation has a lower standard deviation and is characterized by a PDF that is nearly symmetrical around zero. As an indicator of the contribution to the total SGS dissipation we calculate the mean normalized by the total viscous dissipation (M/ε) and the standard deviation (M/σ). The relative support of the PDF is characterized by the standard deviation normalized by the total viscous dissipation (σ/ε). These statistics are shown in Fig. 9 and are summarized in Table 1 for all the Eddy Capturing methods discussed in this paper. The viscous dissipation is defined as: $\varepsilon = \nu \langle 2S_{ij}S_{ij} \rangle$. We can see that the mean of the coherent and total SGS dissipation are of the same order while the mean of the incoherent SGS dissipation is an order of magnitude less. This shows that the majority of the SGS dissipation in LES is due to the coherent structures in the SGS field.

The idea of the SCLES methodology is to model the effect of the coherent and incoherent parts of the SGS separately. It is proposed that the character of the coherent SGS can be inferred from the coherent resolved field and that this information can be used to model the coherent SGS. The incoherent SGS would then be modeled using a stochastic model that would introduce equal amounts of forward and back-scatter. Currently, the physical relationships between the coherent structures in the resolved and unresolved fields have not been quantified and are the subject of ongoing research efforts. It is clear from this example (Fig. 9) that the effort to quantify these physical relationships could benefit the LES community by providing the ba-

sis for more effective coherent structure based subgrid scale models.

The major hurdle to implementing this kind of SCLES approach is the need to know the wavelet threshold ϵ for CVS compression to find $\bar{u}_{>cv_s}$ at each time step. The SCLES method also retains the two major drawbacks of the classical LES method. First there is too much coherency in the SGS field and second is it not temporally adaptive which limits its use in the class of problems dominated by temporally changing physical characteristics. These drawbacks are addressed in the CVS approach but as discussed above the computational cost of CVS is believed to be prohibitive for high Reynolds number turbulent flows. In the next section we will introduce the Stochastic Coherent Adaptive Large Eddy Simulation method that attempts to combine the strengths of LES and CVS.

Stochastic Coherent Adaptive Large Eddy Simulation

We now propose a novel approach called the Stochastic Coherent Adaptive Large Eddy Simulation (SCALES) method which takes advantage of both the CVS and LES methods. With the SCALES method the threshold ϵ of the wavelet filter is chosen such that the minimum number of modes is used to calculate the flow to a specified precision. Only the most dynamically important modes are retained, given the resources available. Note that the threshold used in SCALES could be substantially larger than in CVS, giving a larger compression and making SCALES cost effective for simulating high Re number flows. Note, however, that in SCALES (unlike CVS) some coherent modes will be neglected and the subgrid scales will not have purely Gaussian statistics. The relationship be-

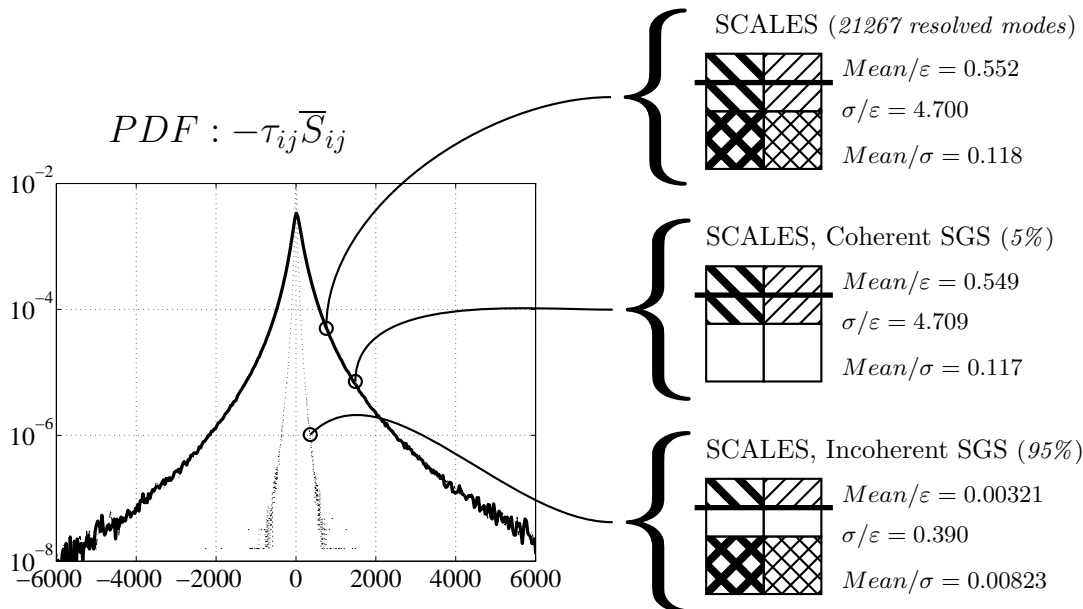


Fig. 10 SCALES subgrid scale dissipation for homogeneous turbulence field F_{256} . Wavelet filter using LI6 wavelets is used.

tween the SCALES methodology and other methods is best presented in terms of the coherency diagram of a turbulent field. In Fig. 6 the horizontal lines of separation on the coherency diagram for DNS, CVS and SCALES are shown. The DNS line is at $\epsilon = 0$ which is the same as no filter. The CVS line is where the field is divided with the coherent structures in the resolved field and the incoherent (Gaussian) residual in the subgrid field. The SCALES line is at a higher ϵ implying that for SCALES the resolved field is made up of coherent structures but the residual subgrid field is made up of both coherent and incoherent parts.

In Fig. 10 we show the probability density function of the SGS dissipation ($-\tau_{ij}\bar{S}_{ij}$) for the SGS field from a wavelet filter applied in the SCALES range to the DNS field F_{256} . Also shown are the coherent and incoherent SGS dissipation. By comparing the normalized means of the SGS dissipation in the three cases (along the right edge of Fig. 10 and summarized in Table 1) we can see that the coherent SGS accounts for the majority of the full SGS dissipation, even though they make up a small percentage of the modes in the full subgrid field. So, as in SCLES, the SGS stress in SCALES must be modeled by a combination of a deterministic model for the coherent part of the SGS stress and a stochastic SGS model for the incoherent part of the SGS stress. What we have gained with SCALES over SCLES is a method that is fully adaptive.

Wavelet Direct Numerical Simulation

To perform a DNS of a turbulent flow the grid and the numerical method must resolve all the physical characteristics of the flow from the characteristic length scale of the domain down to the Kolmogorov length scale. It can be argued that any computation done to capture modes that are below the Kolmogorov

length scale is unnecessary. The dynamically adaptive wavelet collocation method, described in the next section, allows the local error of a simulation to be controlled within order ϵ . This property is used to perform WDNS calculations of turbulent flows. We will present WDNS of two dimensional flows around a cylinder. Figure 6 shows how WDNS relates to DNS, CVS and SCALES. To sum up, WDNS employs an adaptive wavelet method with a small ϵ threshold such that there is wavelet compression of the resolved field, yet all the modes from the characteristic length scale of the domain down to the Kolmogorov length scale are still resolved.

table

Dynamically Adaptive Wavelet Collocation Method

In this section we briefly describe a novel adaptive wavelet computational technique^{3-5, 23, 24}. This technique is ideally suited to the simulation of turbulence since wavelets adapt the numerical resolution naturally to the localized turbulent structures that exist at all wave numbers in fully developed turbulence. Thus, the wavelet approach satisfies Pope's criterion for an ideal LES cited earlier. The wavelet collocation method takes advantage of the fact that wavelets are localized in both space and scale, and as a result, functions with localized regions of sharp transition are well compressed using wavelet decomposition. The adaptation is achieved by retaining only those wavelets, whose coefficients are greater than an *a priori* given threshold (ϵ). Thus, high resolution computations are carried out only in those regions, where sharp transitions occur. With this adaptation strategy, a solution is obtained on a near optimal grid, *i.e.* far fewer grid points are needed for wavelets than for conventional

	LES	SCLES	CVS	SCALES
% Compression	99.8732% ($K_c=16$)	99.8732%	95.0%	99.8732%
% CVS Compression		95.0%	95.0%	95.0%
SGS dissipation				
Mean/ ϵ	0.761	0.761	0.0947	0.552
σ/ϵ	2.457	2.457	1.795	4.700
Mean/ σ	0.310	0.310	0.0527	0.118
Coherent SGS dissipation				
Mean/ ϵ		0.752		0.549
σ/ϵ		2.481		4.709
Mean/ σ		0.303		0.117
Incoherent SGS dissipation				
Mean/ ϵ		0.00892		0.00321
σ/ϵ		0.663		0.390
Mean/ σ		0.0135		0.00823

Table 1 Comparison of SGS dissipation for LES, CVS, SCLES and SCALES. ($\epsilon = \langle 2\nu S_{ij} S_{ij} \rangle$)

finite-difference, finite-element, or spectral methods. By varying the threshold parameter ϵ this method can be used to implement any of the wavelet based methods discussed above, namely WDNS, CVS or SCALES. The dynamically adaptive wavelet collocation algorithm has already been successfully applied to the solution of thermoacoustic wave propagation problems^{23,25}, combustion problems^{3,4}, fluid-structure interaction problems²⁴, viscoelastic flows^{26,27}, and the compaction phenomenon in poro-viscoelastic matrix.²⁸

Let us briefly outline the main features of the numerical method. Details can be found in Refs. 3–5. In the wavelet collocation method there is a one-to-one correspondence between grid points and wavelets, which makes calculation of nonlinear terms simple and allows the grid to adapt automatically and dynamically to the solution by adding or removing wavelets. Very briefly, at each time step we take the wavelet transform of the solution, remove all wavelets with coefficient magnitude less than a threshold ϵ , and then reconstruct the solution. It can be shown that the L_∞ error of this approximation is bounded by ϵ . To account for the evolution of the solution over one time step we add the nearest neighbor wavelet coefficients in position and scale. Since each wavelet corresponds to a single grid point this procedure allows the grid to automatically follow the evolution of the solution in position and scale. We use second generation wavelets²², which allow the order of the wavelet (and hence of the numerical method) to be easily varied. The method has a computational complexity $O(N)$, where N is the number of wavelets retained in the calculation (*i.e.* those wavelets with coefficients greater than ϵ plus nearest neighbors).

In summary, the dynamically adaptive wavelet collocation method is an adaptive, variable order method for solving partial differential equation with localized structures that change their location and scale in space and time. Because the computational grid automatically adapts to the solution (in position and scale), we do not have to know *a priori* where the regions of high gradients or structures exist. In the results pre-

sented in the next section the dynamically adaptive wavelet collocation method has been combined with the Brinkman penalization method^{29,30} to define solid structures in the domain and a new adaptive wavelet collocation multilevel elliptic solver³⁰ to solve the Poisson equation for pressure at each time step.

Results

Computational Complexity

figure

We begin with a series of simulations of the impulsively started flow through a tightly packed cylinder array over a large range of Reynolds numbers, $3 \times 10^1 < Re < 10^5$. To model a large array of cylinders (such as found in the tube bundle of a heat exchanger) we consider one periodic cell where the ratio of cylinder separation to diameter $P/D = 1.5$. The Reynolds number is defined in the usual way as $Re = UD/\nu$, where $U = |\mathbf{U}|$ is the imposed mean flow which is at angle of 45° to the array. We ensure the boundary layer is fully resolved by setting the smallest grid spacing $\Delta x_{\min} = Re^{-1/2}/6$, *i.e.* six points across the boundary layer or Taylor scale $\lambda = Re^{-1/2}$. Each simulation is performed until $t = 1$, by which time the boundary layer is completely formed and trailing vortices begin to appear. The goal of this investigation is to determine how \mathcal{N} (number of active grid points), and overall complexity $(\mathcal{N}/\Delta t)$ scale with Reynolds number. We will verify the claim that adaptive wavelet techniques are well-suited to calculating intermittent high Reynolds number flows.

Figure 11 shows the vorticity and adapted grid at $Re = 3 \times 10^4$. The vorticity is very smooth, and shows no sign of instability or Gibb's oscillation associated with the discontinuity at the surface of the obstacle. The grid is fine only in the thin boundary layer of width $\lambda \approx Re^{-1/2} \approx 0.01$. For an L_∞ -error of 10^{-4} we require only 93 893 grid points, which corresponds to a compression ratio of 25. In particular, there are few points in the interior of the cylinder beyond the skin-depth of thickness about 0.05. This result demonstrates that our approach gives smooth vorticity and a

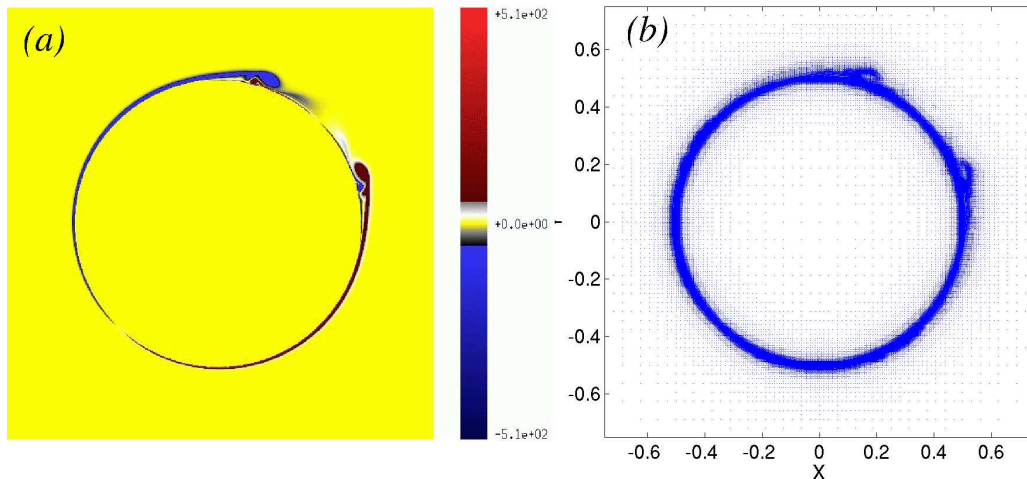


Fig. 11 Two-dimensional periodic cylinder array at $Re = 30000$ at $t = 1$. (a) Vorticity. (b) Adapted grid.

sparse grid even at relatively large Reynolds numbers.

In Figure 12 the ability of the adaptive wavelet collocation method to automatically concentrate the grid in the areas where intermittent energetic structures exist is shown. Since turbulence becomes increasingly intermittent at high Reynolds numbers the adaptive wavelet collocation method should become increasingly efficient as Reynolds number increases. We now check this claim by measuring how \mathcal{N} (number of active wavelets or grid points), compression ratio, time step and overall computational complexity scale with Reynolds number. Figure 12 (a) and (b) show that the number of active grid points and the compression ratio scale like $\lambda \propto Re^{1/2}$, while 12 (d) shows that computational complexity scales like Re . These results support the original claim, since intermittency scales roughly like λ . Note that the overall complexity of the wavelet calculation increases much more slowly than the usual naive scaling estimate of $Re^{9/4}$ for two-dimensional turbulence based on the Kolmogorov scale, or $Re^{3/2}$ based on λ . Furthermore, the scaling law is constant over five orders of magnitude. We might expect, however, that for $Re > 10^6$ (when the boundary layer itself becomes turbulent) the scaling law may change. This will be the subject of future investigation.

figure

Fixed cylinder at $Re = 3000$

For our final example we consider the impulsively started flow around a cylinder at $Re = 3000$. This example shows the accuracy of our method in calculating the singular start-up flow, and the sensitivity of our adaptive wavelet collocation method to strong gradients in the flow. Since we are only interested in the initial flow, we use doubly-periodic boundary conditions and a large domain of size $[-10, 10] \times [-10, 10]$ with a maximum resolution of 6144^2 (which corresponds to $\lambda/5.6$). We maintain a CFL criterion of

1, which gives a time step of about $\Delta t = 2 \times 10^{-3}$.

We show a close-up of the vorticity in Fig. 13. The vorticity field is very similar to Koumoutsakos & Leonard's³¹ equivalent figure 21, and shows fine vortical structure in the downstream boundary layer. The computational grid (not shown) exhibits the same fine adaptivity of the other cases, with few points in the interior of the cylinder.

In figure 14 we compare our drag curve with the short-time asymptotic result of Bar-Lev & Yang³² and the vortex method result of Koumoutsakos & Leonard.³¹ The agreement is excellent, even during the early $t^{-1/2}$ drag singularity. The close match between the curves is especially interesting since the methods are entirely different: Koumoutsakos & Leonard use a vortex method to resolve the vorticity equation, while we use an adaptive high-order finite difference technique to resolve the Navier–Stokes equations in velocity–pressure form. In their paper, Koumoutsakos & Leonard show that previous efforts at simulating this flow were unable to capture the short time singularity, or the plateau and peak shape between $t = 1$ to $t = 2$.

It is interesting to compare the number of computational elements used in the wavelet and vortex methods. In our case these elements are wavelets, and in Koumoutsakos & Leonard's case they are vortices. At $t = 3.0$ we use 4.3×10^4 wavelets (corresponding to a compression ratio of about 880 times), compared with 3.8×10^5 vortices used in the vortex method (*i.e.* almost 9 times fewer computational elements). It therefore appears that the wavelet method is significantly more efficient (in terms of the number of computational elements) than the vortex method. We must remember, however, that the computational cost could be higher per element for wavelets than for vortices.

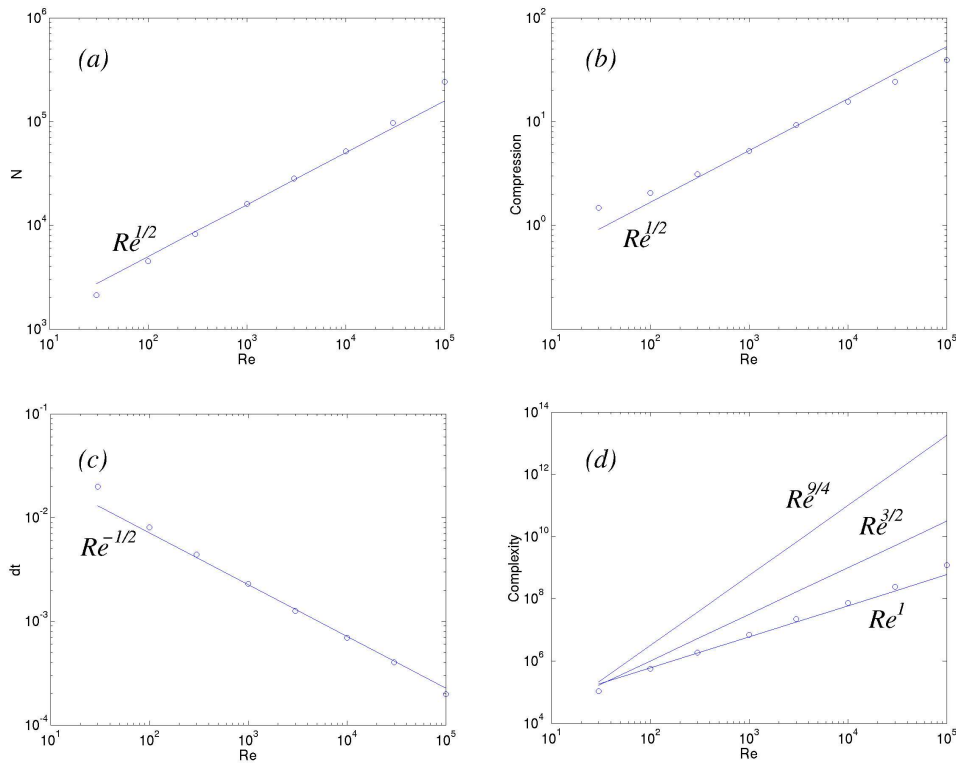


Fig. 12 Scaling for tightly packed cylinder array. (a) Number of active grid points. (b) Compression ratio. (c) Time step. (d) Complexity compared with naive scaling based on the Kolmogorov scale $\eta = Re^{-3/4}$ (which gives $Re^{9/4}$ in two dimensions), and the Taylor scale λ (which gives $Re^{3/2}$ in two dimensions).

Conclusions

In this paper we have presented the theoretical basis for a new method for simulating turbulent flows called Stochastic Coherent Adaptive Large Eddy Simulation (SCALES) that attempts to combine the strengths of CVS and LES. The SCALES methodology uses the idea of wavelet threshold filtering the turbulent field as in CVS⁶, but in SCALES the wavelet filter threshold is increased so only the most energetic part of the coherent vortices are simulated in the resolved field. We have shown in this work that with both LES filtering and SCALES filtering the residual SGS field contains both coherent and incoherent parts. Also we have shown that the total subgrid stress dissipation in both LES and SCALES is dominated by a small number of coherent modes in the SGS field and that given the same compression ratio the SCALES method will result in a significantly lower level of subgrid scale dissipation that needs to be modeled in comparison to LES.

This paper introduces a novel Coherency Diagram of a turbulent field that is useful in understanding the physical relationships between different Large Eddy capturing methods. The Coherency Diagram is used to present the physical relationships between Direct Numerical Simulation, LES, and VLES, which use Fourier Filtering and are non-adaptive, and WDNS, CVS and SCALES, that use wavelet filtering and are fully adap-

tive.

This paper also presents an adaptive wavelet collocation method that can be used to implement any of the wavelet based methods discussed in this paper, namely WDNS, CVS and SCALES. The method combines Brinkman penalization (to define solid structures) with an adaptive wavelet collocation method (to dynamically adapt the computational grid) to solve the Navier–Stokes equations. This method also employs a new adaptive wavelet collocation multilevel elliptic solver³⁰ to solve the Poisson equation for pressure at each time step. Two dimensional results of WDNS have been presented that show that computational complexity scales like Re .

Acknowledgements

The authors would like to thank Dr. Thomas Gatski at NASA Langley for his support of this work through a NASA GSRP fellowship for the first author of this paper. Partial support for the second author (O. V. Vasilyev) was provided by the National Science Foundation under grants No. EAR-0242591 and ACI-0242457. N. Kevlahan gratefully acknowledges financial support from NSERC and the use of SHARCNET’s computer facilities in carrying out calculations reported in this article. We would also like to thank Dr. David A. Yuen at the University of Minnesota Supercomputing Institute for his support of this work.

References

- ¹P. Moin and J. Kim. Tackling turbulence with supercomputers. *Scientific American*, January, 1997.
- ²J. Jimenez and P. Moin. The minimal flow unit in near-wall turbulence. *J. Fluid Mech.*, 225:213–2406, 1991.
- ³O. V. Vasilyev and C. Bowman. Second generation wavelet collocation method for the solution of partial differential equations. *J. Comp. Phys.*, 165:660–693, 2000.
- ⁴O. V. Vasilyev. Solving multi-dimensional evolution problems with localized structures using second generation wavelets. *Int. J. Comp. Fluid Dyn.*, Special issue on high-resolution methods in Computational Fluid Dynamics, 17(2):151–168, 2003.
- ⁵N.K.-R. Kevlahan and O. V. Vasilyev. An adaptive wavelet method for fluid-structure interaction at high reynolds numbers. Submitted to *Phys. Fluids*, 2003.
- ⁶M. Farge, K. Schneider, and N. Kevlahan. Non-Gaussianity and coherent vortex simulation for two-dimensional turbulence using an adaptive orthogonal wavelet basis. *Phys. Fluids.*, 11(8):2187–2201, 1999.
- ⁷P. A. Durbin and B. A. Pettersson Reif. *Statistical Theory and Modeling for Turbulent Flows*. Wiley, 2001.
- ⁸G. H. Cottet and P. D. Koumoutsakos. *Vortex Methods: Theory and Applications*. Cambridge Univ Press, 2000.
- ⁹C. Canuto, M. Y. Hussaini, A. Quarteroni, and T. A. Zang. *Spectral Methods in Fluid Dynamics*. Springer Ser. Comput. Phys., 1987.
- ¹⁰M. Lesieur and O. Metais. New trends in large-eddy simulations of turbulence. *Ann. Rev. Fluid Mech.*, 28:45–82, 1996.
- ¹¹C. Meneveau and J. Katz. Scale-invariance and turbulence models for large-eddy simulation. *Ann. Rev. Fluid Mech.*, 32:1–32, 2000.
- ¹²P. Moin. Advances in large eddy simulation methodology of complex flows. *Int. J. Heat Fluid Flow*, 23:710–720, 2002.
- ¹³J. Jimenez, A. Wray, P. Saffman, and R. Rogallo. The structure of intense vorticity in isotropic turbulence. *J. Fluid Mech.*, 225:65–90, 1993.
- ¹⁴D. A. Goldstein, O.V. Vasilyev, A.A. Wray, and R.S. Rogallo. Evaluation of the use of second generation wavelets in the coherent vortex simulation approach. In *Proceedings of the 2000 Summer Program*, pages 293–304. Center for Turbulence Research, 2000.
- ¹⁵M. Farge, G. Pellegrino, and K. Schneider. Coherent vortex extraction in 3d turbulent flows using orthogonal wavelets. *Physical Review Letters*, 87(5), 2001.
- ¹⁶M. Farge and K. Schneider. Coherent vortex simulation (CVS), a semi-deterministic turbulence model using wavelets. *Flow, Turbulence and Combustion*, 66:393–426, 2001.
- ¹⁷A. Vincent and M. Meneguzzi. The spacial structure and statistical properties of homogeneous turbulence. *J. Fluid Mech.*, 225:1–20, 1991.
- ¹⁸M. Germano, U. Piomelli, P. Moin, and W.H. Cabot. A dynamic subgrid-scale eddy viscosity model. *Phys. Fluids A*, 3(7):1760–1765, 1991.
- ¹⁹S. B. Pope. *Turbulent Flows*. Cambridge University Press, 2000.
- ²⁰U. Piomelli. Large-eddy simulation: achievements and challenges. *Prog. Aero. Sci.*, 35:335–362, 1999.
- ²¹M. Wang and P. Moin. Dynamic wall modeling for large-eddy simulation of complex turbulent flows. *Phys. Fluids*, 14:2043–2051, 2002.
- ²²W. Sweldens. The lifting scheme: A construction of second generation wavelets. *SIAM J. Math. Anal.*, 29(2):511–546, 1998.
- ²³O. V. Vasilyev and S. Paolucci. A fast adaptive wavelet collocation algorithm for multi-dimensional PDEs. *J. Comput. Phys.*, 125:16–56, 1997.
- ²⁴O. V. Vasilyev and N.K.-R. Kevlahan. Hybrid wavelet collocation - Brinkman penalization method for complex geometry flows. *Int. J. Numerical Methods in Fluids*, 40:531–538, 2002.
- ²⁵O. V. Vasilyev and S. Paolucci. A dynamically adaptive multilevel wavelet collocation method for solving partial differential equations in a finite domain. *J. Comput. Phys.*, 125:498–512, 1996.
- ²⁶O. V. Vasilyev, D. A. Yuen, and S. Paolucci. The solution of PDEs using wavelets. *Computers in Phys.*, 11(5):429–435, 1997.
- ²⁷O. V. Vasilyev, Yu. Yu. Podladchikov, and D. A. Yuen. Modeling of viscoelastic plume-lithosphere interaction using adaptive multilevel wavelet collocation method. *Geophys. J. Int.*, 147(3):579–589, 2001.
- ²⁸O. V. Vasilyev, Yu. Yu. Podladchikov, and D. A. Yuen. Modeling of compaction driven flow in poro-viscoelastic medium using adaptive wavelet collocation method. *Geophys. Res. Lett.*, 25(17):3239–3242, 1998.
- ²⁹N. Kevlahan and J.-M. Ghidaglia. Computation of turbulent flow past an array of cylinders using a spectral method with Brinkman penalization. *Eur. J. Mech./B*, 2001. To appear.
- ³⁰O. V. Vasilyev and N. K.-R. Kevlahan. An adaptive multilevel wavelet collocation method for elliptic problems. Submitted to *J. Comp. Phys.*, 2003.
- ³¹P. Koumoutsakos and A. Leonard. High-resolution simulations of the flow around an impulsively started cylinder using vortex methods. *J. Fluid Mech.*, 296:1–38, 1995.
- ³²M. Bar-Lev and H.T. Yang. Initial flow field over an impulsively started circular cylinder. *J. Fluid Mech.*, 72:625–647, 1975.

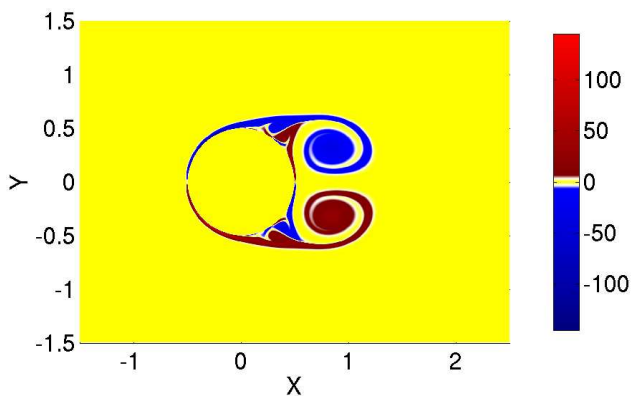


Fig. 13 Vorticity field around a two-dimensional fixed cylinder at $Re = 3000$, $t = 3.0$.

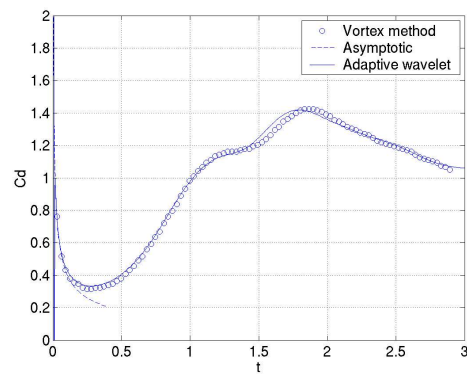


Fig. 14 Drag curve for the impulsively started cylinder at $Re = 3000$ compared to the short time asymptotic result of Bar-Lev & Yang,³² and the vortex method results of Koumoutsakos & Leonard.³¹